



High capacity surface route discharge at the potassium-O₂ electrode

Yuhui Chen^a, Zarko P. Jovanov^a, Xiangwen Gao^a, Jingyuan Liu^a, Conrad Holc^a, Lee R. Johnson^{b,*}, Peter G. Bruce^{a,*}

^a Departments of Materials and Chemistry, Parks Road, University of Oxford, OX1 3PH, UK

^b School of Chemistry and GSK Carbon Neutral Laboratory for Sustainable Chemistry, University of Nottingham, NG7 2TU, UK

ARTICLE INFO

Keywords:

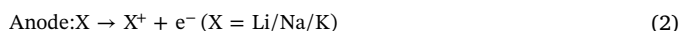
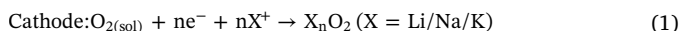
Metal-air
Potassium-oxygen
Oxygen reduction

ABSTRACT

Discharge by a surface route at the cathode of an aprotic metal-O₂ battery typically results in surface passivation by the non-conducting oxide product. This leads to low capacity and early cell death. Here we investigate the cathode discharge reaction in the potassium-O₂ battery and demonstrate that discharge by a surface route is not limited to growth of thin (< 10 nm) metal oxide layers. Electrochemical analysis and in situ Raman spectroscopy confirmed that the product of the cathode reaction is a combination of KO₂ and K₂O₂, depending on the applied potential. Use of the low donor number solvent, acetonitrile, allows us to directly probe the surface route. Rotating ring-disk electrode, electrochemical quartz crystal microbalance and scanning electron microscope characterisations clearly demonstrate the formation of a thick > 1 μm product layer, far in excess of that possible in the related lithium-O₂ battery. These results demonstrate a high-capacity surface route in a metal-O₂ battery for the first time and the insights revealed here have significant implications for the design of the K-O₂ battery.

1. Introduction

Aprotic metal-O₂ batteries have been the focus of intense research due their prospective application as a battery system for long-range electric vehicles and other energy demanding applications [1–6]. During the discharge process of a typical aprotic metal-O₂ battery, an alkali metal anode, e.g. Li/Na/K, is oxidized, which produces alkali ions that take part in an oxygen reduction reaction (ORR) at the cathode forming superoxide, peroxide or other oxide species, as shown below.



The Li-O₂ battery is the most promising due to a theoretical specific energy of 3500 Wh kg^{−1} based on the discharge product Li₂O₂ [1]. The Na-O₂ battery has a specific energy of 1105 Wh kg^{−1} or 1602 Wh kg^{−1} based on the formation of NaO₂ and Na₂O₂ on discharge, respectively [7]. The K-O₂ battery has a specific energy of 935 Wh kg^{−1} and is believed to form KO₂ [8]. Although the specific energy of the Na-O₂ and K-O₂ batteries are notably lower than that of the Li-O₂ battery, both demonstrated much smaller polarisation and significantly higher energy efficiency during discharge and charge. The voltage gap between discharge and charge is ~100 mV for Na-O₂ and ~50 mV for K-O₂, compared to 1 V for Li-O₂ [8–10]. This variation is attributed to the different type of discharge product, superoxide in Na-O₂/K-O₂ versus

peroxide in Li-O₂. Recently the chemistry at the cathode in the aprotic Li-O₂ battery has been established and two competitive routes have been demonstrated on discharge, the solution route and the surface route [11,12]. The former results in growth of Li₂O₂ as a chemical step from solution, leading to a high capacity and rate capability, while the latter forms a Li₂O₂ film on the electrode surface, resulting in low rates and capacities. Similar mechanisms are known to occur in other aprotic metal-O₂ batteries [13,14].

When discharging a metal-O₂ battery by a surface route, conductivity of the newly formed phase is critical. However, the importance and origin of conductivity in metal-O₂ batteries remains under debate. Curtiss and Amine et al. have proposed that Li₂O₂ deposits have a superoxide-like character [15–17], resulting in a quasi-semiconductor like material. Siegel et al. have suggested conductivity within the bulk by formation of hole and electron polarons and defects in the form of site vacancies [18,19]. In practice, the Li₂O₂ film formed on discharge is restricted to a thickness of 7 nm due to its low electric conductivity, 10^{−12}–10^{−11} S cm^{−1} at 100 °C [20,21]. As a result, surface route discharge in the Li-O₂ battery typically results in a low capacity and premature cell death and therefore the solution route is overwhelmingly desired [1]. In addition, similar studies of the Na-O₂ system also suggest that conductivity of NaO₂ is limited and that discharge by a surface route is not a dominant discharge pathway [14,22], although calculation shows that NaO₂ has a higher conductivity than LiO₂ [23].

* Corresponding authors.

E-mail addresses: lee.johnson@nottingham.ac.uk (L.R. Johnson), peter.bruce@materials.ox.ac.uk (P.G. Bruce).

<https://doi.org/10.1016/j.jelechem.2018.03.041>

Received 31 July 2017; Received in revised form 9 February 2018; Accepted 20 March 2018

Available online 21 March 2018

1572-6657/ © 2018 The Authors. Published by Elsevier B.V. This is an open access article under the CC BY-NC-ND license (<http://creativecommons.org/licenses/by-nc-nd/4.0/>).

Since the K-O₂ battery was reported in 2013 [8], only a few studies of the system have been reported and the discharge mechanism in the K-O₂ battery remains poorly understood [24–27]. Here we explore discharge in the K-O₂ battery using solvents that are expected to induce a surface route. We show that capacity, far in excess of that for a thin film, can be passed during discharge by a surface route in the K-O₂ battery. We confirm an electrodeposition route by rotating ring-disk electrode (RRDE) and electrochemical quartz crystal microbalance (EQCM) methods and characterise the discharge product using in-situ surface-enhanced Raman spectroscopy (SERS). We highlight that this is the first report of a surface route discharge mechanism in aprotic metal-O₂ chemistry, able to form a thick, high capacity, surface layer. Finally, we propose some possible origins of this effect and consider the implications for the K-O₂ battery.

2. Results and discussions

Fig. 1a shows cyclic voltammograms (CVs) for dioxygen reduction in presence of K⁺ and Li⁺ in CH₃CN. CH₃CN was selected as the solvent as it is known to favour a surface-confined reaction rather than a solution reaction with dissolved intermediates, while also possessing high conductivity and limited Raman peaks. While both CVs are similar in shape, it is immediately evident that the peak current and charge passed in the K-O₂ system far exceed that of the Li-O₂ system. It is also worth noting that the ratio of charge passed on oxidation over charge passed on reduction is far higher in the K-O₂ system, 0.90, than that in the Li-O₂ system, 0.18. This high ratio suggests that the reduction product in the K-O₂ system can be easily oxidized, unlike the Li-O₂ system, and implies a high degree of chemical reversibility. As discussed above, oxygen reduction to form alkali oxides in CH₃CN (low donor number, DN) is known to form insulating solids at the electrode surface resulting in low currents and low charge passed. The fact that the K-O₂ system does not fit into this theory is intriguing and to date unexplored. We highlight that similar CVs are published in the literature but their significance has not been realised [8].

2.1. Dioxygen reduction in K-O₂

CVs for the ORR in CH₃CN with varying K⁺ amounts are shown in Fig. 1b. With TBA⁺ ions only, the well-known quasi-reversible redox couple O₂/O₂^{•−} is observed, Eq. (3) [28,29]. Upon addition of K⁺ ions in place of TBA⁺, a new peak occurs at positive potentials and this shifts positive in potential and increases in magnitude as the concentration of the alkali ion is increased. The new peak has characteristics consistent with formation of an insulating product (peak followed by a drop to near zero current) and the formation is at the expense of the original reduction peak. The positive shift of the onset potential is consistent with stabilisation of the superoxide by the K⁺ ion, similar to that proposed in other metal-O₂ systems, Eq. (4) [13,30].

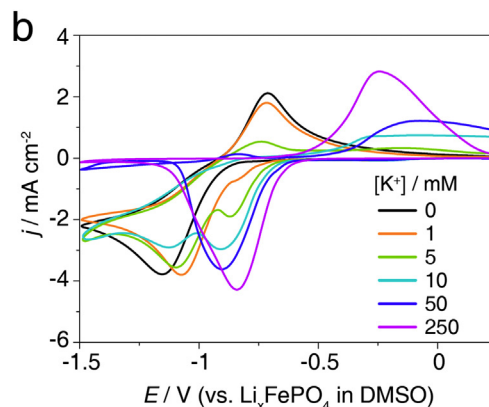
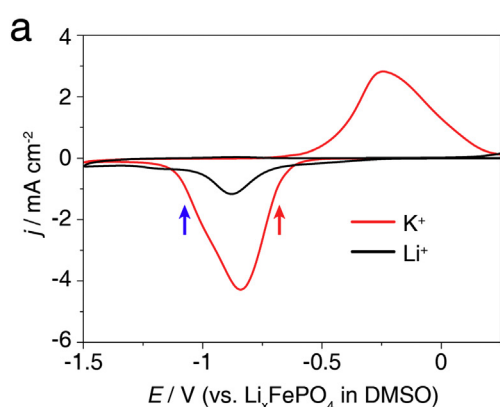


Fig. 1. Cyclic voltammetry (CV) of dioxygen in the presence of K⁺, and Li⁺ ions in CH₃CN. (a) Comparison of the voltammetric response with 250 mM Li⁺ or K⁺ ions only. Arrows indicate the potentials at which SERS spectra were recorded. (b) Voltammograms recorded with increasing K⁺ concentration where the total salt concentration is maintained at 250 mM using a tetrabutylammonium, TBA⁺, salt. Measurements were performed in O₂ saturated solutions with 250 mM of the relevant triflate salt at a Au electrode at 100 mV s^{−1}.



Unlike Li-O₂, disproportionation of KO₂ can be ruled out on the grounds of thermodynamics ($\Delta G_{f,\text{KO}_2} < \Delta G_{f,\text{K}_2\text{O}_2}$). A calculation of the free energy change can be found in the Supplementary Information. Close inspection of the reduction peak for K-O₂, Fig. 1a, shows that it consists of two peaks, with one at higher and one at lower potentials, where the latter is a shoulder on the negative side of the former. We note that this second lower potential reduction peak is not due to the original O₂/TBA redox couple as no TBA⁺ is present in the Fig. 1a and an analysis of soluble O₂^{•−} discussed later does not show any correlation of this peak with a solution phase O₂^{•−}. It is well established in the Li-O₂ field that LiO₂ can be reduced to the peroxide and this peak suggests a similar process is occurring in K-O₂, where KO₂ is further reduced to K₂O₂, Eq. (5). Indeed, electrochemical reduction of KO₂ is likely to occur in all systems at some potential [6,31]. These data suggest that the two peaks are due to the formation of KO₂ and K₂O₂. To confirm this, in situ SERS was recorded while holding the potential at a high voltage, −0.7 V (vs. Li_xFePO₄ in DMSO) and a low voltage, −1.1 V (vs. Li_xFePO₄ in DMSO), where we expect to form mainly superoxide and peroxide, respectively (Fig. 2). A table showing the assignment of all peaks in the spectra and a table of standard Raman peak positions for common compounds in the K-O₂ battery are provided in the Supplementary Information. When holding the potential at −0.7 V, a new peak occurred at 1132 cm^{−1} consistent with the formation of KO₂, i.e. a blue shift from the free O₂^{•−} position (1108 cm^{−1}) towards the bulk crystal KO₂ position (1145 cm^{−1}). When stepping the potential to −1.1 V, the peak for KO₂ disappeared and a new peak occurred at 816.3 cm^{−1}, which is in the region we expect to see a peroxide O–O stretch, indicating that this peak is due to formation of K₂O₂.

While interesting, the results thus far cannot explain why significantly more charge is passed in K-O₂ in comparison to Li-O₂. The charge passed in the K-O₂ system far exceeds that expected for an electrodeposited thin film based on the conductivity of either KO₂ or K₂O₂ although a passivating limit is evident [32]. This indicates conductivity or partial solubility. However, both KO₂ and alkali peroxides are considered insulating, although debate exists in the literature regarding the conductivity of KO₂, and both have little or no solubility in this solvent [20,32,33]. We note that the effect can also be observed in other solvents such as dimethyl sulfoxide (DMSO) and diethylene glycol dimethyl ether (diglyme), Fig. S3. By holding at a low potential to drive reduction of O₂ to K₂O₂, very similar amounts of capacity were consumed to form the surface film, suggesting the products in three solvents had very similar conductivities. Here we only use these solvents as a means of testing our proposed theory. Ether based electrolytes are

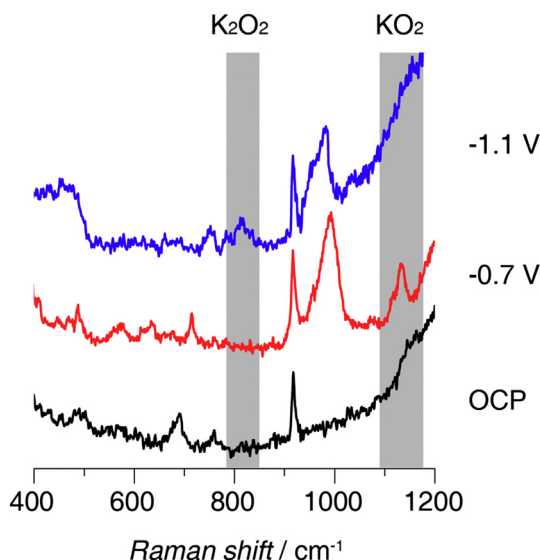


Fig. 2. Showing in situ SERS during ORR with K^+ in CH_3CN . Spectra collected at a Au electrode during O_2 reduction in the presence of 250 mM KTFA at -0.7 V and -1.1 V (vs. Li_xFePO_4 in DMSO), as indicated by the matching coloured markers in the CVs, Fig. 1a. (Black) open circuit potential. Shaded region shows the position of the superoxide and peroxide peaks.

currently used in $K-O_2$ cells [8], but DMSO is not a viable solvent for a practical battery and is unstable against metallic K.

2.2. Solution versus surface routes

In the following section we explore the solubility of reaction intermediates by RRDE voltammetry and the growth of surface products by EQCM for $K-O_2$. In tandem, these two techniques provide a unique ability to observe both solution and surface routes in metal- O_2 systems.

The RRDE results, Fig. 3a, are similar to the static voltammograms, and are consistent with the surface dominant reaction expected in CH_3CN . The ring current indicates the amount of soluble superoxide in the system and as previously shown [11], this is limited in $Li-O_2$. The data shows that the solubility of KO_2 in CH_3CN is also low and at this level it cannot explain the large charge passed during reduction, i.e., the product of the reduction is not simply dissolving into solution and avoiding surface passivation. This demonstrates that solubility cannot

explain the increased charge associated with $K-O_2$. Fig. 3b shows EQCM results for $Li-O_2$ and $K-O_2$, respectively, and both show an increase in mass roughly proportional to the charge passed. This confirms the formation of a surface film on reduction, rather than formation of soluble products, which is consistent with RRDE results. Most significantly, more mass is electrodeposited in $K-O_2$ in comparison to $Li-O_2$. This unequivocally demonstrates that the increased charge passed in the $K-O_2$ system results in the formation of a thick film of product on the electrode surface and that this forms by a surface route, which is unique in the field of aprotic metal- O_2 . Due to the mixed product and small solubility of KO_2 we cannot confirm the nature of the product from the EQCM data, i.e., by relating $\Delta mass/\Delta charge$.

Fig. 4 shows scanning electron microscopy (SEM) images of the discharge product formed during dioxygen reduction in $K-O_2$ at a Au wire. Notably, the product film formed appears continuous and free from holes, Fig. 4a, consistent with an electrochemical growth. Fig. 4b shows an etched cross-section at the Au wire, which shows a thick deposit on the electrode surface. Fig. 4c shows a section of the film, which has delaminated from the underlying electrode during drying and unmistakably demonstrates the thickness of the film formed. Raman and FTIR characterisation of this film are shown in Fig. S4, and these show that the film mainly consists of KO_2 . We do not expect to see K_2O_2 ex situ as this will likely decompose to KO_2 in the O_2 atmosphere of the cell (see discussion in the Supplementary Information).

To further explore the growth mechanism of the superoxide-like product in $K-O_2$, electrochemical impedance spectra were recorded during discharge at a planar Au electrode, Fig. 5 and Fig. S5. In all systems at the earlier stages of discharge we observed a single semi-circle in the Nyquist plot with a tail at lower frequencies. This is a typical EIS response of the positive electrode charge transfer reaction in metal- O_2 batteries [34]. The resistance, R , of the single semi-circle is associated with the charge transfer reaction and therefore, conductivity of the surface film. Considering first the $Li-O_2$ system, while R is initially low, this rapidly increases after only 2.5 mC cm^{-2} of charge (c.a. 35 s), Fig. S6, and is accompanied by a large voltage polarisation in the D.C. measurement. In contrast, for the same amount of charge passed, R does not change significantly in the $K-O_2$ system.

R steadily increases during discharge from c.a. $10\text{ k}\Omega$ to $18\text{ k}\Omega$ during the first 175 s of discharge, indicating the potassium oxide film formed introduces a gradually increasing resistance to charge transfer, but not to a point of complete passivation. As the discharge approaches completion the EIS spectrum does not show a clear RC response for an electron transfer, indicating that the conductivity is now insufficient to maintain the discharge, i.e., the thick potassium oxide film has now

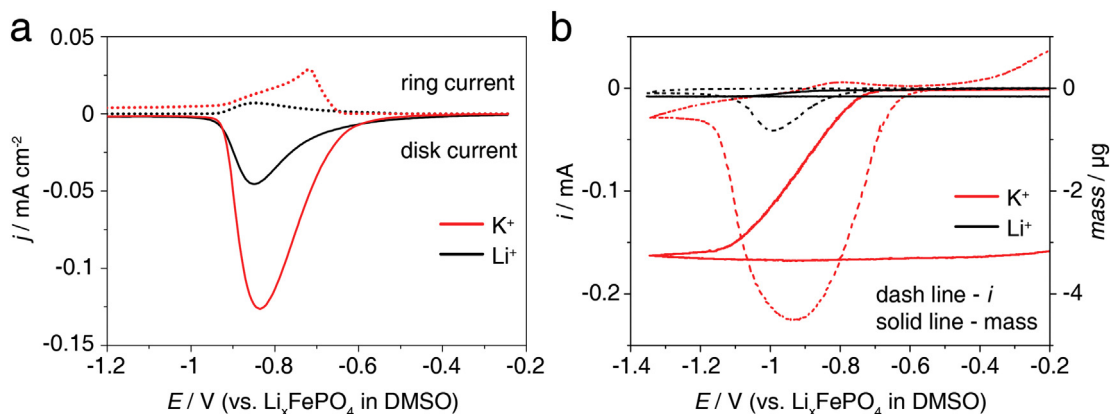


Fig. 3. RRDE and EQCM measurements of O_2 reduction showing significant surface route discharge with K^+ in comparison to Li^+ containing electrolytes. (a) Polarisation curves obtained in O_2 saturated CH_3CN containing 250 mM $LiTFA$ (black) or $KTFA$ (red). The RRDE was a 5 mm diameter Au disk with a Au ring and the rotation rate was 2000 RPM. (b) Cyclic voltammetry of oxygen reduction in O_2 saturated CH_3CN containing 250 mM $LiTFA$ (black) and $KTFA$ (red) in CH_3CN (dashed lines) and EQCM response (solid lines). Measurements were recorded at gold coated quartz crystals at 20 mV s^{-1} . (For interpretation of the references to colour in this figure legend, the reader is referred to the web version of this article.)

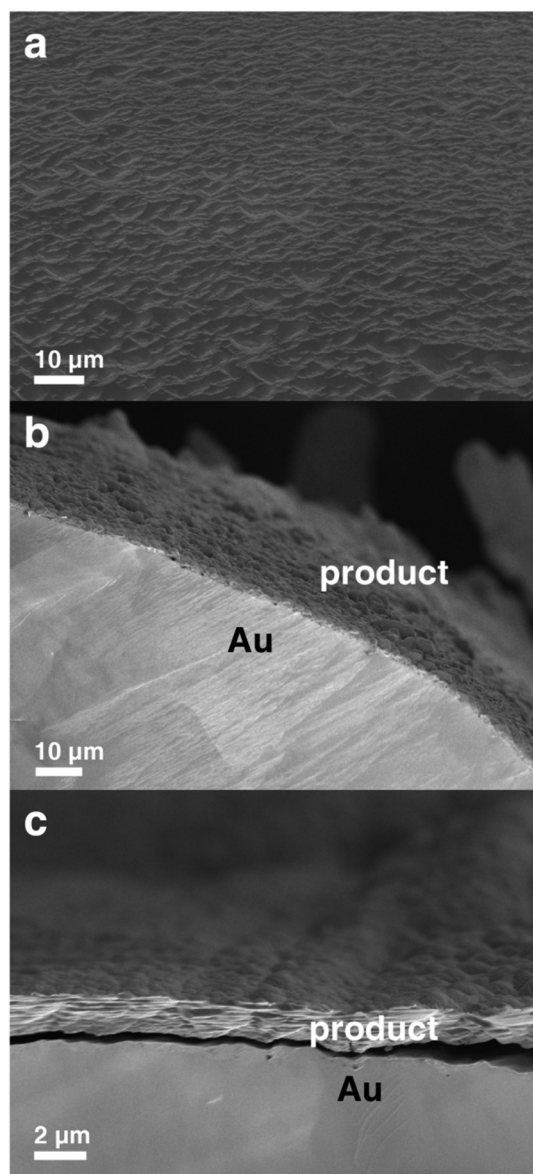


Fig. 4. Morphology of the discharge product of the K-O₂ reaction at a Au wire electrode. SEM images showing (a) the surface of and (b, c) cross sections of the resulting discharge product formed on a Au wire. The Au wire was discharged at -1.1 V (vs. Li_xFePO₄ in DMSO) in O₂ saturated 250 mM KTFA in CH₃CN in a 3-electrode glass cell.

passivated the surface. This happens at a capacity of c.a. 10 mC cm^{-2} of charge, and may be due to passivation by KO₂ and K₂O₂ or some products from side-reactions, which will preferentially form at negative potentials. These data, in conjunction with the ECQM data demonstrate that in the K-O₂ system, the discharge product formed by a surface route displays enhanced conductivity compared to other alkali ion metal-O₂ discharge products and forms by a classical electrodeposition mechanism.

2.3. Rationalising conductivity in K-O₂

Our results strongly suggest the presence of a conducting phase during discharge in K-O₂ and as mentioned, this has been shown, if not discussed previously [8]. However, this increasing conductivity is intriguing. One possibility is significant side-reaction with the solvent. But we note that K-O₂ does not readily react with CH₃CN and that we observe a similar effect in other solvents, making this an unlikely

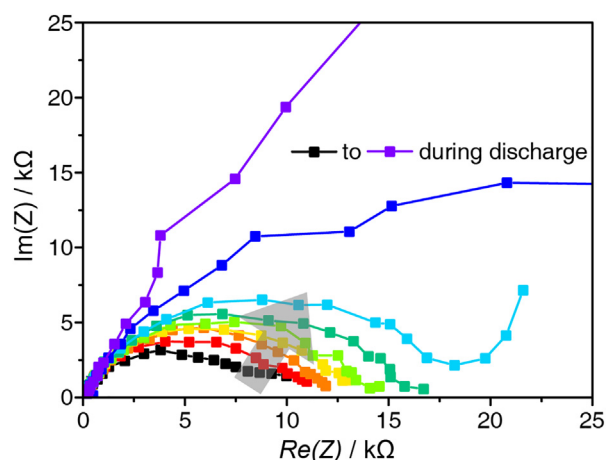


Fig. 5. Nyquist plot showing the limited increase in charge transfer resistance during K-O₂ discharge. Measurements were performed at $50 \mu\text{A cm}^{-2}$ in O₂-saturated 250 mM KTFA CH₃CN at a planar Au electrode. The load curve for the discharge is shown in Fig. S5 in the SI.

scenario. A study of the conductivity of alkali oxides showed them to be effectively insulating, which fails to explain the effects observed here [22]. However, we note that conflicting reports exist for the conductivity of KO₂, which has been described as a room temperature semiconductor, whereas other reports suggest a room temperature conductivity of $10^{-13} \text{ S cm}^{-1}$ [32,35]. It has been proposed that one of the primary factors controlling conductivity in these oxides is the ability of the dioxygen to take varying oxidation states, i.e., O₂²⁻, O₂¹⁻, O₂⁰, the relative formation energy of such sites and consequently their concentration [18]. Their occurrence within the peroxide or superoxide lattice provides routes to both hole polarons and electron polarons (charged polarisation within the lattice) [22]. For example, a superoxide like dioxygen in a peroxide lattice effectively creates a hole due to the missing electron. Conversely, inclusion of a peroxide in a superoxide lattice forms an electron conductor. As KO₂ is more stable than K₂O₂, see Supplementary Information, retaining superoxide like character in the oxide layer may be favourable resulting in the formation of a mixed product (various oxygen valences) and consequently, increasing concentration of polaron charge carriers. Finally, it should be noted that we cannot rule out conductivity in non-crystalline phases, such as amorphous oxides and grain boundaries.

3. Conclusion

Here we show for the first time that in an aprotic metal-O₂ battery system, a large discharge capacity can be obtained from a surface discharge route. While the origin of this effect remains elusive, the implications are significant, as a new class of metal-O₂ battery could be realised where the challenge of obtaining a high capacity is entirely different from that in the Li-O₂ and Na-O₂ systems. While the latter rely on partial solubility or redox mediators to promote large capacities and high rates, these appear implicit in the chemistry of the K-O₂ battery cathode reaction. These insights should be carefully considered in the design and performance of K-O₂ cells.

Acknowledgements

P.G.B. is indebted to the EPSRC and the RCUK Energy programme including SUPERGEN Energy Storage Hub EP/L019469/1 for financial support. L.R.J. gratefully acknowledges support from the University of Nottingham's Beacon in Propulsion Futures.

Appendix A. Supplementary data

Supplementary data to this article can be found online at <https://doi.org/10.1016/j.jelechem.2018.03.041>. Additional data has been deposited in the OxfordResearch Archive at <https://doi.org/10.5287/bodleian:1RYk6Ka0>.

References

- [1] D. Aurbach, B.D. McCloskey, L.F. Nazar, P.G. Bruce, Advances in understanding mechanisms underpinning lithium–air batteries, *Nature Energy* 1 (2016) 16128.
- [2] K.M. Abraham, Prospects and limits of energy storage in batteries, *J. Phys. Chem. Lett.* 6 (5) (2015) 830–844.
- [3] J. Lu, Y.J. Lee, X. Luo, K.C. Lau, M. Asadi, H.H. Wang, S. Brombosz, J. Wen, D. Zhai, Z. Chen, D.J. Miller, Y.S. Jeong, J.B. Park, Z.Z. Fang, B. Kumar, A. Salehi-Khojin, Y.K. Sun, L.A. Curtiss, K. Amine, A lithium–oxygen battery based on lithium superoxide, *Nature* 529 (7586) (2016) 377–382.
- [4] C.L. Bender, D. Schroder, R. Pinedo, P. Adelhelm, J. Janek, One- or two-electron transfer? The ambiguous nature of the discharge products in sodium–oxygen batteries, *Angew. Chem. Int. Ed.* 55 (15) (2016) 4640–4649.
- [5] H. Yadegari, Q. Sun, X. Sun, Sodium–oxygen batteries: a comparative review from chemical and electrochemical fundamentals to future perspective, *Adv. Mater.* 28 (33) (Sept. 7 2016) 7065–7093.
- [6] D. Krishnamurthy, H.A. Hansen, V. Viswanathan, Universality in nonaqueous alkali oxygen reduction on metal surfaces: implications for Li–O₂ and Na–O₂ batteries, *ACS Energy Letters* 1 (1) (2016) 162–168.
- [7] R. Pinedo, D.A. Weber, B. Bergner, D. Schröder, P. Adelhelm, J. Janek, Insights into the chemical nature and formation mechanisms of discharge products in Na–O₂ batteries by means of OperandoX-ray diffraction, *J. Phys. Chem. C* 120 (16) (2016) 8472–8481.
- [8] X. Ren, Y. Wu, A low-overpotential potassium–oxygen battery based on potassium superoxide, *J. Am. Chem. Soc.* 135 (8) (2013) 2923–2926.
- [9] P. Hartmann, C.L. Bender, M. Vracar, A.K. Duerr, A. Garsuch, J. Janek, P. Adelhelm, A rechargeable room-temperature sodium superoxide (NaO₂) battery, *Nat. Mater.* 12 (3) (2013) 228–232.
- [10] B.D. McCloskey, J.M. Garcia, A.C. Luntz, Chemical and electrochemical differences in nonaqueous Li–O₂ and Na–O₂ batteries, *J. Phys. Chem. Lett.* 5 (7) (2014) 1230–1235.
- [11] L. Johnson, C. Li, Z. Liu, Y. Chen, S.A. Freunberger, P.C. Ashok, B.B. Praveen, K. Dholakia, J.-M. Tarascon, P.G. Bruce, The role of LiO₂ solubility in O₂ reduction in aprotic solvents and its consequences for Li–O₂ batteries, *Nat. Chem.* 6 (12) (2014) 1091–1099.
- [12] K.H. Xue, E. McTurk, L. Johnson, P.G. Bruce, A.A. Franco, A comprehensive model for non-aqueous lithium air batteries involving different reaction mechanisms, *J. Electrochem. Soc.* 162 (4) (2015) A614–A621.
- [13] L. Lutz, W. Yin, A. Grimaud, D. Alves Dalla, M. Tang Corte, L. Johnson, E. Azaceta, V. Sarou-Kanian, A.J. Naylor, S. Hamad, J.A. Anta, E. Salager, R. Tena-Zaera, P.G. Bruce, J.M. Tarascon, High capacity Na–O₂ batteries: key parameters for solution-mediated discharge, *J. Phys. Chem. C* 120 (36) (2016) 20068–20076.
- [14] P. Hartmann, M. Heinemann, C.L. Bender, K. Graf, R.-P. Baumann, P. Adelhelm, C. Heiliger, J. Janek, Discharge and charge reaction paths in sodium–oxygen batteries: does NaO₂ form by direct electrochemical growth or by precipitation from solution? *J. Phys. Chem. C* 119 (40) (2015) 22778–22786.
- [15] J. Yang, D. Zhai, H.-H. Wang, K.C. Lau, J.A. Schlueter, P. Du, D.J. Myers, Y.-K. Sun, L.A. Curtiss, K. Amine, Evidence for lithium superoxide-like species in the discharge product of a Li–O₂ battery, *Phys. Chem. Chem. Phys.* 15 (11) (2013) 3764–3771.
- [16] K.C. Lau, J. Lu, X. Luo, L.A. Curtiss, K. Amine, Implications of the unpaired spins in Li–O₂ battery chemistry and electrochemistry: a minireview, *ChemPlusChem* 80 (2) (2015) 336–343.
- [17] K.C. Lau, R.S. Assary, P. Redfern, J. Greeley, L.A. Curtiss, Electronic structure of lithium peroxide clusters and relevance to lithium–air batteries, *J. Phys. Chem. C* 116 (45) (2012) 23890–23896.
- [18] M.D. Radin, D.J. Siegel, Charge transport in lithium peroxide: relevance for rechargeable metal–air batteries, *Energy Environ. Sci.* 6 (8) (2013) 2370.
- [19] F. Tian, M.D. Radin, D.J. Siegel, Enhanced charge transport in amorphous Li₂O₂, *Chem. Mater.* 26 (9) (2014) 2952–2959.
- [20] O. Gerbig, R. Merkle, J. Maier, Electron and ion transport in Li₂O₂, *Adv. Mater.* 25 (22) (2013) 3129–3133.
- [21] V. Viswanathan, K.S. Thygesen, J.S. Hummelshøj, J.K. Nørskov, G. Girishkumar, B.D. McCloskey, A.C. Luntz, Electrical conductivity in Li₂O₂ and its role in determining capacity limitations in non-aqueous Li–O₂ batteries, *J. Chem. Phys.* 135 (21) (2011) 214704.
- [22] S. Yang, D.J. Siegel, Intrinsic conductivity in sodium–air battery discharge phases: sodium superoxide vs sodium peroxide, *Chem. Mater.* 27 (11) (2015) 3852–3860.
- [23] B. Lee, J. Kim, G. Yoon, H.-D. Lim, I.-S. Choi, K. Kang, Theoretical evidence for low charging overpotentials of superoxide discharge products in metal–oxygen batteries, *Chem. Mater.* 27 (24) (2015) 8406–8413.
- [24] A. Eftekhari, Z. Jian, X. Ji, Potassium secondary batteries, *ACS Appl. Mater. Interfaces* 9 (5) (2016) 4404–4419.
- [25] N. Xiao, X. Ren, M. He, W.D. McCulloch, Y. Wu, Probing mechanisms for inverse correlation between rate performance and capacity in K–O₂ batteries, *ACS Appl. Mater. Interfaces* 9 (5) (2016) 4301–4308.
- [26] X. Ren, K.C. Lau, M. Yu, X. Bi, E. Kreidler, L.A. Curtiss, Y. Wu, Understanding side reactions in K–O₂ batteries for improved cycle life, *ACS Appl. Mater. Interfaces* 6 (21) (2014) 19299–19307.
- [27] X. Ren, M. He, N. Xiao, W.D. McCulloch, Y. Wu, Greatly enhanced anode stability in K-oxygen batteries with an in situ formed solvent- and oxygen-impermeable protection layer, *Adv. Energy Mater.* 7 (1) (2017).
- [28] C.O. Laoire, S. Mukerjee, K.M. Abraham, E.J. Plichta, M.A. Hendrickson, Influence of nonaqueous solvents on the electrochemistry of oxygen in the rechargeable lithium–air battery, *J. Phys. Chem. C* 114 (19) (2010) 9178–9186.
- [29] D.L. Maricle, W.G. Hodgson, Reduction of oxygen to superoxide anion in aprotic solvents, *Anal. Chem.* 37 (12) (1965) 1562–1565.
- [30] J.S. Hummelshøj, A.C. Luntz, J.K. Nørskov, Theoretical evidence for low kinetic overpotentials in Li–O₂ electrochemistry, *J. Chem. Phys.* 138 (3) (2013) 034703.
- [31] D. Krishnamurthy, H.A. Hansen, V. Viswanathan, Universality in nonaqueous alkali oxygen reduction on metal surfaces: implications for Li–O₂ and Na–O₂ batteries, *ACS Energy Lett.* 1 (1) (2016) 162–168.
- [32] O. Gerbig, R. Merkle, J. Maier, Electrical transport and oxygen exchange in the superoxides of potassium, rubidium, and cesium, *Adv. Funct. Mater.* 25 (17) (2015) 2552–2563.
- [33] X. Gao, Z.P. Jovanov, Y. Chen, L.R. Johnson, P.G. Bruce, Phenol-catalyzed discharge in the aprotic lithium–oxygen battery, *Angew. Chem. Int. Ed.* 56 (23) (2017) 6539–6543.
- [34] J. Højberg, B.D. McCloskey, J. Hjelm, T. Vegge, K. Johansen, P. Norby, A.C. Luntz, An electrochemical impedance spectroscopy investigation of the overpotentials in Li–O₂ batteries, *ACS Appl. Mater. Interfaces* 7 (7) (2015) 4039–4047.
- [35] A.U. Khan, S.D. Mahanti, Collective electron effects of O^{2−} in potassium superoxide, *J. Chem. Phys.* 63 (6) (1975) 2271–2278.